British Journal of Cancer

ARTICLE

Cellular and Molecular Biology

Neuropeptide Y, a paracrine factor secreted by cancer cells, is an independent regulator of angiogenesis in colon cancer

Debanjan Chakroborty[1,2,3,4,5,7], Sandeep Goswami[1,3,4,7], Hao Fan[1], Wendy L. Frankel[1,2], Sujit Basu[1,2,6] and Chandrani Sarkar[1,2,3,4,5]✉

BACKGROUND: Resistance to anti-angiogenic therapies targeting vascular endothelial growth factor-A (VEGF-A) stems from VEGF-A independent angiogenesis mediated by other proangiogenic factors. Therefore identifying these factors in colon adenocarcinoma (CA) will reveal new therapeutic targets.
METHODS: Neuropeptide Y (NPY) and Y2 receptor (Y2R) expressions in CA were studied by immunohistochemical analysis. Orthotopic HT29 with intact VEGF-A gene and VEGF-A knockdown (by CRISPR/Cas9 gene-editing technique) HT29 colon cancer-bearing mice were treated with specific Y2R antagonists, and the effects on angiogenesis and tumour growth were studied. The direct effect of NPY on angiogenesis and the underlying molecular mechanism was elucidated by the modulation of Y2R receptors expressed on colonic endothelial cells (CEC).
RESULTS: The results demonstrated that NPY and Y2R are overexpressed in human CA, orthotopic HT29, and most interestingly in VEGF-A-depleted orthotopic HT29 tumours. Treatment with Y2R antagonists inhibited angiogenesis and thereby HT29 tumour growth. Blocking /silencing Y2R abrogated NPY-induced angiogenic potential of CEC. Mechanistically, NPY regulated the activation of the ERK/MAPK signalling pathway in CEC.
CONCLUSIONS: NPY derived from cancer cells independently regulates angiogenesis in CA by acting through Y2R present on CEC. Targeting NPY/Y2R thus emerges as a novel potential therapeutic strategy in CA.

British Journal of Cancer (2022) 127:1440–1449; https://doi.org/10.1038/s41416-022-01916-1

BACKGROUND

Advanced colon adenocarcinoma (CA) shows increased vascularisation (angiogenesis, i.e., increased microvessel density) and intratumoral expression of proangiogenic factors that are associated with poor prognosis [1, 2]. Studies indicate that the vascular endothelial growth factor-A (VEGF-A) pathway is critical in promoting angiogenesis during tumour growth and progression. Therefore, anti-VEGF-A agents targeting the VEGF-A-mediated proangiogenic pathways were developed and approved to treat advanced CA patients [3, 4]. Unfortunately, although anti-VEGF-A anti-angiogenic agents initially showed promise in treating metastatic CA, recent results indicate increasing failure of these drugs in a subset of patients [5–7]. Activation or upregulation of alternative proangiogenic signalling pathways within the tumour is one of the prominent adaptive mechanisms that confer evasive resistance to these therapies [8]. Accordingly, alternative angiogenic pathways have been observed in various anti-VEGF-A resistant cancers [9, 10].

The enteric nervous system and neuromediators have long been linked to gastrointestinal (GI) tract diseases like inflammatory bowel diseases (IBD) and cancer of the GI tract [11–15]. Among the neuromodulators that play essential roles in the gut, neuropeptide Y (NPY) has been shown to regulate several key functions like gastric motility and electrolyte secretion [16]. NPY is a 36 amino acid residue peptide of the pancreatic polypeptide family, found in the brain, autonomic nervous system and different peripheral tissues, including the colon [17–21]. NPY interacts with a family of G-protein-coupled receptors (GPCR) (Y1, Y2, Y4, Y5 and y6) belonging to the rhodopsin-like superfamily (class1) of receptors, which couple to Gi and thus decrease cAMP accumulation in a variety of cell lines and tissues [16, 17, 21]. Apart from its function in controlling food intake, adiposity and maintenance of the energy homeostasis within the body [14, 16], dysfunction of the NPY or NPY system has been implicated in cardiovascular and GI disorders, including IBD and diabetes [14, 21–24]. Though patients with IBD are more prone to the development of CA in their lifetime [25–27], and NPY plays a significant role in the pathogenesis of IBD, there is no report describing the role of NPY in CA.

We report here that NPY and its Y2 receptor (Y2R) are significantly expressed in human CA tissues and orthotopic human colon cancer

[1]Department of Pathology, The Ohio State University, Columbus, OH 43210, USA. [2]Comprehensive Cancer Center, The Ohio State University, Columbus, OH 43210, USA. [3]Department of Pathology, University of South Alabama, Mobile, AL 36617, USA. [4]Cancer Biology Program, Mitchell Cancer Institute, University of South Alabama, Mobile, AL 36604, USA. [5]Department of Biochemistry and Molecular Biology, College of Medicine, University of South Alabama, Mobile, AL 36688, USA. [6]Division of Medical Oncology, Department of Internal Medicine, The Ohio State University, Columbus, OH 43210, USA. [7]These authors contributed equally: Debanjan Chakroborty, Sandeep Goswami.
✉email: csarkar@southalabama.edu

Received: 9 March 2022 Revised: 11 July 2022 Accepted: 12 July 2022
Published online: 28 July 2022

in athymic mice. NPY, by acting through Y2R regulates colon cancer growth and progression by promoting angiogenesis. Furthermore, NPY expression in CA is strongly correlated with disease progression as metastatic CA tissues show the highest expression of NPY. Most interestingly, in a VEGF-A knockdown HT29 (VEGF-A KO HT29) colon cancer orthotopic model where VEGF-A was knocked down in HT29 cells using the CRISPR/Cas9 technique, simulating conditions in which VEGF-A induced angiogenesis is not the central proangiogenic pathway as is seen in many advanced CA patients, we found NPY to be highly elevated in tumour tissues which also correlated with increased angiogenesis and tumour growth. Furthermore, targeting Y2R by specific antagonists in these orthotopic colon cancers significantly reduced angiogenesis and tumour growth, indicating that NPY is an independent regulator of angiogenesis in CA.

MATERIALS AND METHODS

Human tissues

Clinical specimens of various stages of CA from male and female patients, adjacent normal/benign tissue and normal colon tissues were obtained from The Ohio State University tissue archive per institutional IRB guidelines.

Cell culture

HT29 (ATCC, Manassas, VA) and VEGF-A KO HT29 cells were cultured in McCoy's 5A medium, supplemented with 10% FBS (Life Technologies, CA). VEGF-A KO HT29 cells were generated using the CRISPR/Cas9 genome editing system [28]. Briefly, gRNA plasmids PC590.VEGF-A.g3 (40% cleavage activity) [TTCTGCTGTCTTGGGTGCATNGG] and PC590.VEGF-A.g7 (32% cleavage activity) [CACGACCGCTTACCTTGGCANGG] were transfected with Cas9 plasmid into HT29 cells. Cells were selected using 2 µg/ml puromycin. After single-cell cloning and screening of cell colonies by genotyping, hVEGF-A knockout clones were expanded and cryopreserved. Colonic endothelial cells (CEC) (Cell Biologics, IL) were cultured in an endothelial cell medium with growth supplement, antibiotics, and foetal bovine serum. Cultures were maintained at 37 °C in 5% CO_2 in a humidified incubator. Experiments with CEC were performed between passages 3 and 7. All cell lines were validated by short tandem repeat DNA fingerprinting at ATCC and found negative for mycoplasma infection.

Mouse tumour models and treatment

All mouse experiments were performed according to protocols approved by the Institutional Animal Care and Use Committee (IACUC) at The Ohio State University, Columbus, OH. For the development of orthotopic HT29 tumour models, athymic nude mice of both sexes, 6–8 weeks of age, were purchased from Charles River Laboratories, Wilmington, MA and models were created as described previously [29, 30]. Briefly, mice were anaesthetised with ketamine/xylazine (100 mg/10 mg, i.p.), and HT29 or VEGF-A KO HT29 cells (1×10^6 cells in 50 µL medium) were transplanted to the caecal wall from the serosal side using a 30-gauge needle through a small incision made on the abdominal wall at the ventrolateral side. The caecum was returned to the abdominal cavity, and the wound was closed in one layer with proline 4.0 surgical sutures [29, 30]. Animals with tumours of similar size in the caecum were divided randomly into control and treatment groups. 11 mice per group were used to ensure adequate power.Treatment group mice were treated either with BIIE0246 (2 mg/kg × 7 days, i.p.) [31] or JNJ5207787 (30 mg/kg × 7 days, i.p.) [32]. Mice were sacrificed on day 8. At necropsy, tumours were harvested from the primary site, and the tumour weight was recorded and compared among different study groups. No blinding was done during xenograft experiments.

Immunohistochemistry/immunofluorescence staining

Upon collection, tissues were snap-frozen or were fixed in 10% neutral buffered formalin. Formalin-fixed sections were routinely processed for paraffin sectioning. For histology or immunostaining experiments, sections were cut at a thickness of 5 µm, deparaffinized at 65 °C for 15 min, and then hydrated through a series of xylene and alcohol baths before staining. Antigen retrieval was done using sodium citrate buffer (10 mM sodium citrate, 0.05% Tween 20, pH 6.0) in a pre-heat steamer (2100 Antigen Retriever, Electron Microscopy Sciences) for 2 hr. Slides were then allowed to cool for 15 min at room temperature. The tissue sections were then rinsed in phosphate-buffered saline (PBS) and immersed in 3% H_2O_2 for 5 min at room temperature. Thereafter, the sections were incubated with 2.5% normal horse serum (Vector Laboratories, CA) at room temperature for 20 min to block the nonspecific binding sites and were stained for CD31 (Cat# NB100-2284 Novus Biologicals, CO and Cat# AF3628 R&D Systems, MN), Ki67 (Cat# ab15580 Abcam, MA), VEGF-A (Cat# ab1316 Abcam, MA), NPY (Cat# NB600-1094 Novus Biologicals, CO) or Y2R (Cat# SAB4502029 Sigma, MO and Cat# NB110-59978 Novus Biologicals, CO) using ImmPRESS–Ap/ImmPRESS–HRP polymer kit (Vector Laboratories, CA). The slides were finally visualised; stained cells were counted/ scored in a blinded manner by two independent investigators and photographed using Zeiss Axioscope A1 upright light microscope. For NPY and Y2R scoring, a scoring range of 0–12 was used. The percentage of tissue stained was measured on a scale of 0-4 (0 = no stain, 1 = <10% positive staining, 2 = 10–50% positive staining, 3 = 51–80% positive staining and 4 = >80% positive staining). Staining intensity was measured on a scale of 0–3 (0 = no colour reaction, 1 = mild reaction and 3 = intense reaction). The score for each section was calculated by multiplying the two values obtained in order to normalise the heterogeneity of staining and the multifocal nature of the tumour [33]. In situ cell death detection kit (Trevigen, MD) was used to detect apoptosis. The apoptotic index was determined as the ratio between tunnel-positive cells to the total number of cells (Apoptotic Index = DAB-positive cells X100/total no. of cells). Double immunofluorescence, i.e., colocalization studies, were performed with CD31 + Y2R and CD31 + pERK [phospho-p44/42 MAPK (Erk1/2) (Thr202/Tyr204), Cat#4370 Cell Signaling Technology, MA], [phospho-p38 MAPK (Thr180/Tyr182) Cat#4511 Cell Signaling Technology, MA], antibodies. Staining was visualised under a confocal scanning microscope (Zeiss LSM 700), analysed and compared between different groups [29, 30, 34]. The total colocalized (yellow) area (%) was determined using NIH J Image [28, 29].

Western blot analysis

Western blots were performed with phospho-p44/42 MAPK (Erk1/2) (Thr202/Tyr204) Cat#4370 Cell Signaling Technology, MA, total p44/42 MAPK (Erk1/2) Cat#4695 Cell Signaling Technology, MA, phospho-p38 MAPK (Thr180/Tyr182) Cat#4511 Cell Signaling Technology, MA, total p38 MAPK Cat#9212 Cell Signaling Technology, MA, GAPDH Cat#2118 Cell Signaling Technology, MA, Y1R Cat# OABF00442) Aviva System Biology, CA and Y2R Cat# SAB4502029 Sigma, MO and Cat# NB110-59978 Novus Biologicals, CO, antibodies. Briefly, cells were homogenised with RIPA (Boston Bioproducts, MA) containing protease inhibitor cocktail, PMSF and sodium orthovanadate (Sigma, MO). After estimating protein (Bradford protein assay, Bio-Rad Laboratories, CA), equal amounts (40 µg of cell lysates) were electrophoresed using polyacrylamide gel. Bio-Rad Trans-Blot Turbo™ Transfer Pack was used to transfer proteins to 0.2-µm PVDF membranes. The PVDF membranes were pre-blocked with either 5% BSA (for detecting phosphoproteins) or nonfat dried milk in TBS (5%) and then incubated with primary and HRP-conjugated secondary antibodies. Protein molecular weight markers (Precision Plus protein Standards, Bio-Rad Laboratories, CA) run on the same gel were used to determine the molecular weights. Band images were obtained using a C-Digit blot scanner. Representative bands were measured by densitometry (NIH J Image) and compared between the groups. GAPDH served as an internal control [28–30, 34–36].

In vitro cell proliferation assay

Cells were plated onto Nunc 96-well dishes (3000–5000 cells/well in 200 µl growth medium). After settling, cells were washed once with PBS and allowed to grow in reduced serum (0.5%) and growth factor-containing media for 24 hrs. Cells were then treated with NPY alone (100 nM) or in the presence of specific NPY receptor antagonists (BIIE0246, JNJ5207787 or BIBO3304 trifluoroacetate, Tocris) (1 µM) and incubated at 37 °C. After 24 hrs of incubation, Prestoblue™cell viability reagent (20 µl/well, Invitrogen, NY) was added, and cells were further incubated at 37 °C for 30 min. Absorbance was measured at 570 nm experimental and 600 nm reference wavelengths using a BioTek plate reader [36].

Scratch wound assay

For in vitro wound-healing assay, cells were cultured to near confluence in 24-well plates precoated with collagen (2 µg/cm^2), starved for 24 hrs and cell monolayers were then wounded by a p200 pipette tip in one direction

to create a scratch. NPY (100 nM) was added alone or with BIIE0246 or BIBO3304 (1 μM, Tocris, added 1 hr prior to administration of NPY). After the initial scratch, images were taken, and the gap between the two fronts was measured using the microscope scale measurement analysis (D0). The bottom of the wells was marked with a fine tip marker which was used as the reference point for further measurement. Cells were incubated at 37 °C and monitored every 2 hrs under a phase-contrast microscope until complete closure of the wound was observed in the NPY-treated wells. Images were taken from the same field and the gap was calculated in all the groups at the same time point and marked as Dt. Wound closure was calculated by measuring the average distance between the edges of the two migrating columns and expressed as % wound closure [% wound closure = {(D0 − Dt/D0) × 100} where D0 is the initial distance between two migrating cell fronts and Dt is the final distance between two migrating cell fronts and expressed as relative wound closure compared to the NPY-treated group [29, 36, 37].

In vitro cell migration assay

In vitro cell migration assay was performed using the QCM 3-μm endothelial cell migration kit (Millipore, MA). CEC (3×10^5 cells) were seeded on a basement-coated porous insert in the endothelial invasion chamber. Cells were allowed to settle. In the upper chamber, BIBO3304 trifluoroacetate or BIIE0246 (1 μM) was added. NPY was added at a concentration of 100 nM in the upper compartment of the invasion chamber after 1 hr. Cells were allowed to invade through the basal membrane at 37 °C in a 5% CO_2 incubator for 6 hrs. After the incubation, the inserts were taken out, non-migratory cells remaining in the upper chamber were removed with the help of cotton swabs, and the inserts were washed gently with PBS. The lower surface of the invasion chamber was stained with the cell staining solution supplied in the kit. After staining and careful washing, the number of cells that migrated across the coated membrane were visualised under Zeiss Axiovert inverted microscope, counted and photographed with Axiocam. After standardisation and compensation with the untreated control, the number of migrated cells was calculated and compared between different experimental groups [36].

In vitro tubulogenesis assay

In vitro tube formation was assessed using in vitro angiogenesis assay kit (Trevigen, MD) as per the instruction of the manufacturer. Briefly, all the reagents were brought to room temperature before addition. Cultrex Basement Membrane Extract (BME) was thawed in the ice water bath in a refrigerator at 2–4 °C overnight before use, added to the 96-well culture plates and plates were placed at 37 °C for 30–60 min for polymerisation. Starved cells treated either with NPY alone or in the presence of BIIE0246 or BIBO3304 trifluoroacetate were seeded and incubated for 6–12 hrs at 37 °C. Tubule formation was assessed in independent microscopic fields using Zeiss inverted Axiovert microscope. Images were taken and compared between different study groups [36].

Reverse-transcription PCR

Qiagen QIAshredder and a one-step RT-PCR (Qiagen, MD) kit were used for RNA isolation and RT-PCR. PCR was done using a thermocycler (Eppendorf). The primer sequences were: VEGF-A—forward 5′-GAGATGAGCTTCCTACAG CAC-3′, reverse 5′-TCACCGCCTCGGCTTGTCACAT-3′; GADPH—forward 5′-CGA GATCCCTCCAAAATCAA-3′, reverse 5′-TGTGGTCATGAGTCCTTCCA-3′; Y2R—forward 5′-TGTTTTCCTCGTTCCATTGGT-3′, reverse 5′-AATACTCCCGGAAGATG GCC-3′; NPY—forward 5′-TAGGTAACAAGCGACTGGGG-3′, reverse 5′-CAGGGT CTTCAAGCCGAGTT-3′ and Y1R—forward 5′-CTCTTGCTTATGGRGATGTGA-3′, reverse 5′-CTGGAAGTTTTTGTTCAGGAAYCCA-3′ [38–41].

Real-time PCR

RNeasy Mini Kit (Qiagen, MD) was used according to the manufacturer's protocol to isolate total RNA from HT29 and CEC. NanoDrop spectrophotometer (Thermo Fisher Scientific, CA) was then used to determine the RNA concentration. cDNA synthesis was done using RevertAid™ premium first-strand cDNA synthesis system from Thermo Scientific for RT-PCR using oligo dT primers. Real-time PCR was done with SYBER green mixed (catalogue number:K0221, Thermo Fisher Scientific, CA) using QuantStudio™ 3 Real-Time PCR System (Applied Biosystem, MA) using a 96-well format to determine expressions of Y1R, Y2R, Y4R, Y5R and Y6R in the samples using first-strand cDNA as templates. Gene sequences from the GenBank database were used to design the PCR primers. GAPDH expression was the endogenous control. Arbitrary units were used to express the relative expression and the fold change in gene expression was determined by ΔCt method. Real-time PCR for each gene was performed in triplicate [28]. Primers used: Y1R (forward 5′-CCATCG GACTCTCATAGGTTGTC-3′, reverse 5′-GACCTGTACTTATTGTCTCTCATC-3′); Y2R (forward 5′-ACTCCTAGAGGTGAACTGGTCC-3′, reverse 5′-CATGGATC ACCAAGGAGTTGCC-3′); Y4R (forward 5′-ACATTGCCAGGATTCCGTGGAC-3′, reverse 5′-CGTTGGCTTTCTCCTTCTGCCT-3′); Y5R (forward 5′-CCTCAGGT GAAACTCTCTGGCA-3′, reverse 5′-GAGAAGGTCTTTCTGGAGCAGG-3′); Y6R (forward 5′-CTGTCCTACCACCTCACTGATG-3′, reverse 5′-AAAGGGAGGTGG TGAAGAGCAG-3′) and GAPDH (forward 5′-GTCTCCTCTGACTTCAACAGCG-3′, reverse 5′-ACCACCCTGTTGCTGTAGCCAA-3′) (Invitrogen, CA).

siRNA knockdown of Y2R in endothelial cells

siRNA targeting Y2R was purchased from Ambion® Invitrogen™ (siY2R) and diluted in a serum-free medium containing transfection reagents. One day prior to transfection, CEC were plated in 12-well plates. The concentrations of siRNA were optimised to ensure that cell viability was not affected. Upon reaching 60–70% confluence, CEC were transfected with siY2R (10–100 μM) or negative universal control (Ambion® Invitrogen™) by magnetofection using SilenceMag beads following the manufacturer's protocol (OZ Biosciences, France). Knockdown of Y2R in CEC was confirmed by western blot analysis, and siY2R transfected CEC (40 μM) were used for in vitro assays 48 hrs after transfection [28, 29].

Statistical analysis

All statistical analyses were performed in a blinded manner using GraphPad Prism 8 version 8.1.0 (GraphPad Software, San Diego, CA, USA). Differences between independent groups were evaluated by ANOVA for experiments involving more than two groups and by a two-sample *t* test for experiments with two groups. Data are presented as mean ± SEM; $P < 0.05$ was considered significant [28, 29, 36]; all in vitro assays were repeated using three biological replicates.

RESULTS

Overexpression of NPY and Y2R in colon cancer is correlated with disease progression and increased angiogenesis

To investigate the status of NPY and Y2R in de-identified CA tissues collected from both male and female patients of different age groups, we performed immunohistochemistry (IHC). Our IHC results indicated that NPY (dilution 1:200) and its receptor Y2R (dilution 1:200) were significantly upregulated in CA tissues compared to normal colon tissues collected from the same patients, which showed low-to-moderate expressions of both NPY and Y2R. Our results further indicated that expression of NPY in CA strongly correlated with the disease stage, with metastatic CA showing the highest expressions (Fig. 1). Interestingly, in highly metastatic (primarily liver) orthotopic HT29 colon cancer grown in athymic nude mice (Fig. 2a), we observed similar upregulation of NPY (Fig. 2b) and Y2R (Fig. 2c). However, the expressions of NPY and Y2R were low in normal mouse colon tissues (Fig. 2b, c).

Furthermore, a significant increase in the number of microvessels (angiogenesis/CD31 positive vessels) was observed in the CA compared to the normal colon tissues (Fig. 3a, b). Interestingly, a strong positive correlation was evident between angiogenesis and overexpression of NPY in these tissues ($r^2 = 0.8397$) (Fig. 3c). Likewise, in HT29 tumours orthotopically grown in athymic nude mice, significantly increased angiogenesis was noted compared to normal colon tissues (Fig. 3d, e), and NPY expression in the HT29 tumour tissues also showed a strong positive correlation with the intratumoral microvessel density ($r^2 = 0.8175$) (Fig. 3f).

Our studies further indicated that Y2R expression in CA tissues was remarkably upregulated on CD31 positive endothelial cells in these tissues. Confocal microscopy revealed that in both CA (Fig. 3g) and orthotopic HT29 colon cancer (Fig. 3h), Y2R expression was specifically upregulated in colonic endothelial cells (CEC) [colocalization of Y2R and CD31/microvessels].

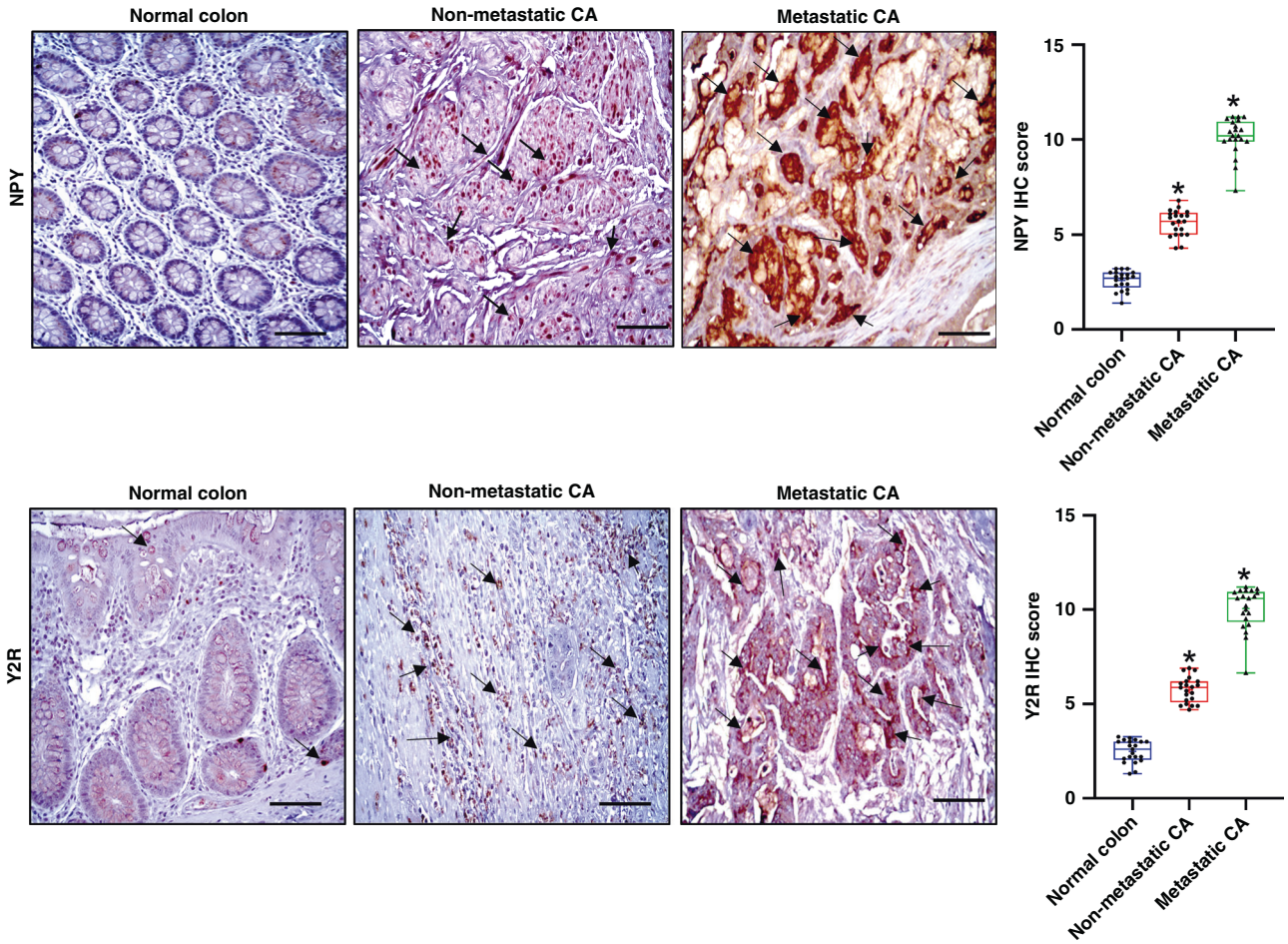

Fig. 1 Expressions of neuropeptide Y (NPY) and its receptor (Y2R) are significantly upregulated in colon adenocarcinoma (CA). Representative immunohistochemistry images showed that NPY and Y2R are significantly overexpressed in non-metastatic and metastatic human CA compared to the normal colon tissues. Box plots showed significant differences in the mean total score for immunohistochemistry between the normal colon and non-metastatic and metastatic CA. Results are expressed as mean ± SEM; CA relative to the normal colon; *$P < 0.01$. Scale bar, 100 μm; $n = 21$ per group.

Y2R antagonists inhibit the growth of orthotopic HT29 colon tumours by inhibiting angiogenesis

Since NPY expression in CA significantly correlated with disease stage and the neovessel numbers in both human CA and orthotopically grown HT29 tumours and Y2R also strongly expressed on tumour endothelial cells in these tissues, we next investigated whether inhibition of Y2R impacted colon cancer growth and progression. Our results indicated that upon treatment with Y2R antagonists, BIIE0246 (2 mg/kg for 7 days) [31] and JNJ5207787 (3 mg/kg for 7 days) [32], there was significant inhibition of HT29 tumour growth (tumour weight) compared to the untreated control group (Fig. 4a). The reduction of tumour growth by Y2R antagonists was accompanied by significant inhibition of angiogenesis or MVD/CD31 expression (CD31: Novus Biologicals, 1:100) (Fig. 4b) and a significant increase in tumour cell apoptosis (tunnel assay) (Fig. 4c) in tumour tissues. However, there was no significant difference in tumour cell proliferation (Ki67: Abcam, 1:50) between Y2R antagonists treated and control groups (Supplementary Fig. S1).

NPY is significantly upregulated in VEGF-A-depleted orthotopic HT29 colon cancer

Next, to simulate a VEGF-A non-responsive or resistant condition, we created a VEGF-A-depleted model of orthotopic HT29 colon cancer where VEGF-A was knocked down in HT29 tumour cells using the CRISPR/CAS9 gene-editing technique. Then VEGF-A knocked out HT29 cells (VEGF-A KO HT29) were orthotopically transplanted to the colon of athymic nude mice. As tumour cells are the major source of VEGF-A, knocking out VEGF-A in HT29 cells significantly reduced VEGF-A in the tumour microenvironment (Supplementary Fig. S2a). VEGF-A knockout in HT29 cells was confirmed by reverse transcription-polymerase chain reaction (RT-PCR) and western blot analysis (Supplementary Fig. S2b). To our surprise, we noted that the VEGF-A KO HT29 orthotopic tumours were also highly metastatic like wild-type HT29 tumours (Supplementary Fig. S3). In orthotopic VEGF-A KO HT29 tumours that showed very low expression of VEGF-A compared to normal HT29 tumours (Supplementary Fig. S2a), we noted significant expressions of both NPY and Y2R as was noted in the wild-type HT29 tumours (Fig. 4d). Furthermore, the tumours were highly angiogenic, and no significant difference in angiogenesis was observed between orthotopic VEGF-A KO HT29 and wild-type HT29 tumours (Fig. 4b, e). NPY in tumour tissues correlated with increased microvessel density (MVD) or CD31 staining or angiogenesis in these tissues (Fig. 4f; $r^2 = 0.5994$). Most importantly, our results demonstrated that inhibition of Y2R with Y2R-specific antagonists, BIIE0246 and JNJ5207787, significantly inhibited angiogenic response and growth (tumour weight) in these VEGF-A KO HT29 tumours (Fig. 4e, g). Tumour cell apoptosis was also significantly increased upon treatment with Y2R

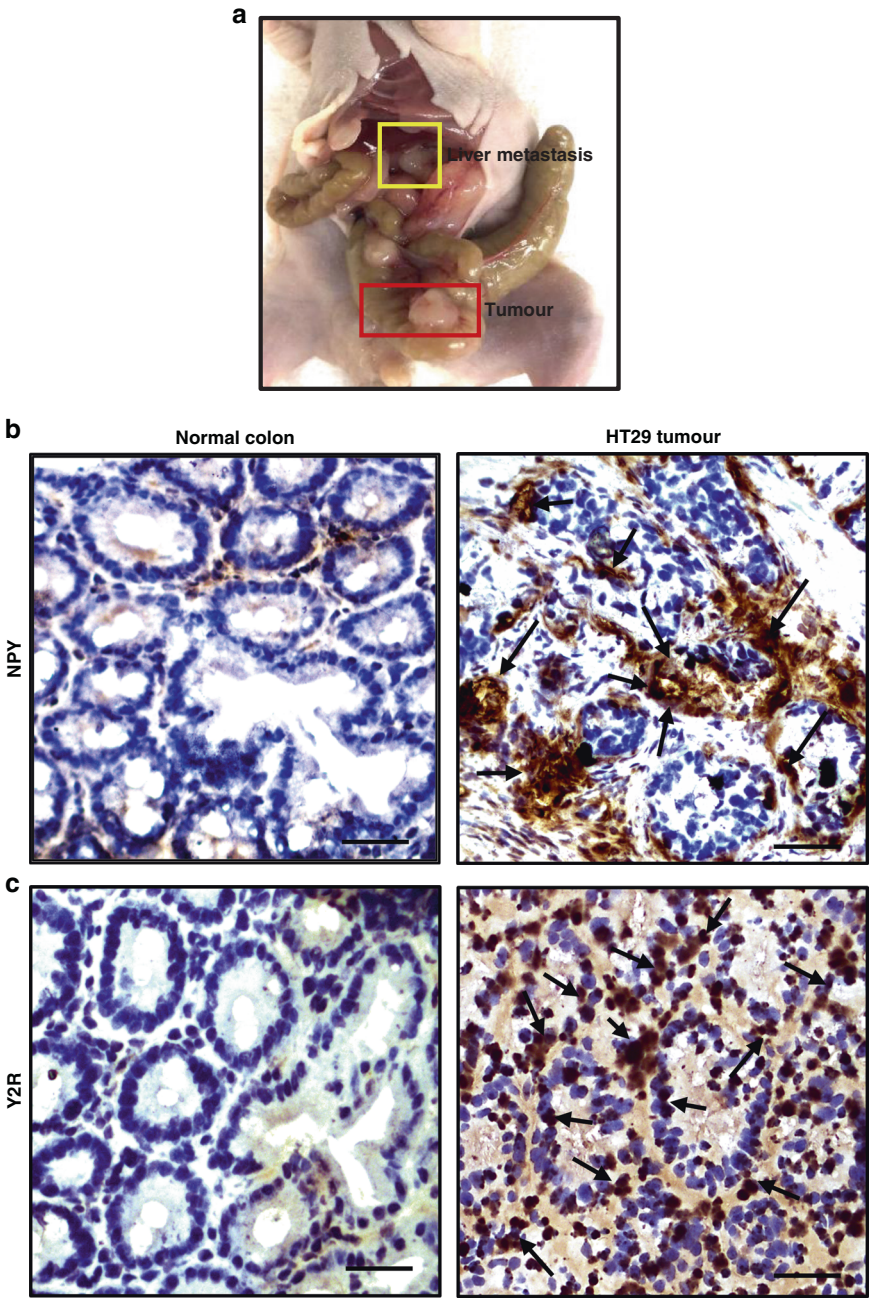

Fig. 2 Neuropeptide Y (NPY) and Y2R are overexpressed in orthotopic HT29 colon cancer. a Highly metastatic orthotopic HT29 colon cancer in athymic nude mice. Representative images of immunohistochemistry show **b** NPY and **c** Y2R expressions in normal mouse colon and HT29 tumour tissues. NPY and Y2R are both overexpressed in metastatic HT29 colon tumours. Normal mouse colon shows low NPY and Y2R expressions. Scale bar, 100 μm; $n = 11$/group; data represent the summary of six or more sections per mouse from each group.

antagonists (Fig. 4h). Similar to wild-type HT29 tumours, no significant difference in tumour cell proliferation (Ki67: Abcam, 1:50) was observed between Y2R antagonists treated and control groups (Supplementary Fig. S4). Together, the results confirmed that targeting Y2R with specific blockers could inhibit colon tumour growth. Most importantly, the results further confirmed that NPY is an independent regulator of angiogenesis in colon cancer.

NPY mediates stimulation of colonic endothelial cells, specifically through Y2R

Our in vivo immunohistochemistry results showed that NPY is upregulated in human CA and orthotopically grown HT29 colon cancer tissues (Figs. 1, 2 and 4). Our in vitro ELISA and RT-PCR results further confirmed that colon cancer cells (wild-type HT29 and VEGF-A KO HT29) were major sources of NPY (Fig. 5a, b). In addition, our western blot and RT-PCR results confirmed that Y1R and Y2R were expressed on CEC (Fig. 5c). qRTPCR results further demonstrated the presence of other NPY receptors (Y4, Y5 and Y6) on HT29 cells and CEC (Supplementary Fig. S5a). Even though Y2R receptors are present on HT29 cells, treatment of these cells with BIIE0246 (1 μM, Tocris) did not have any effect on cell proliferation (Supplementary Fig. S5b).

Proliferation, migration and tubule formation of endothelial cells are essential steps of angiogenesis. Since NPY is synthesised and secreted by colon cancer cells and Y2R is highly expressed on

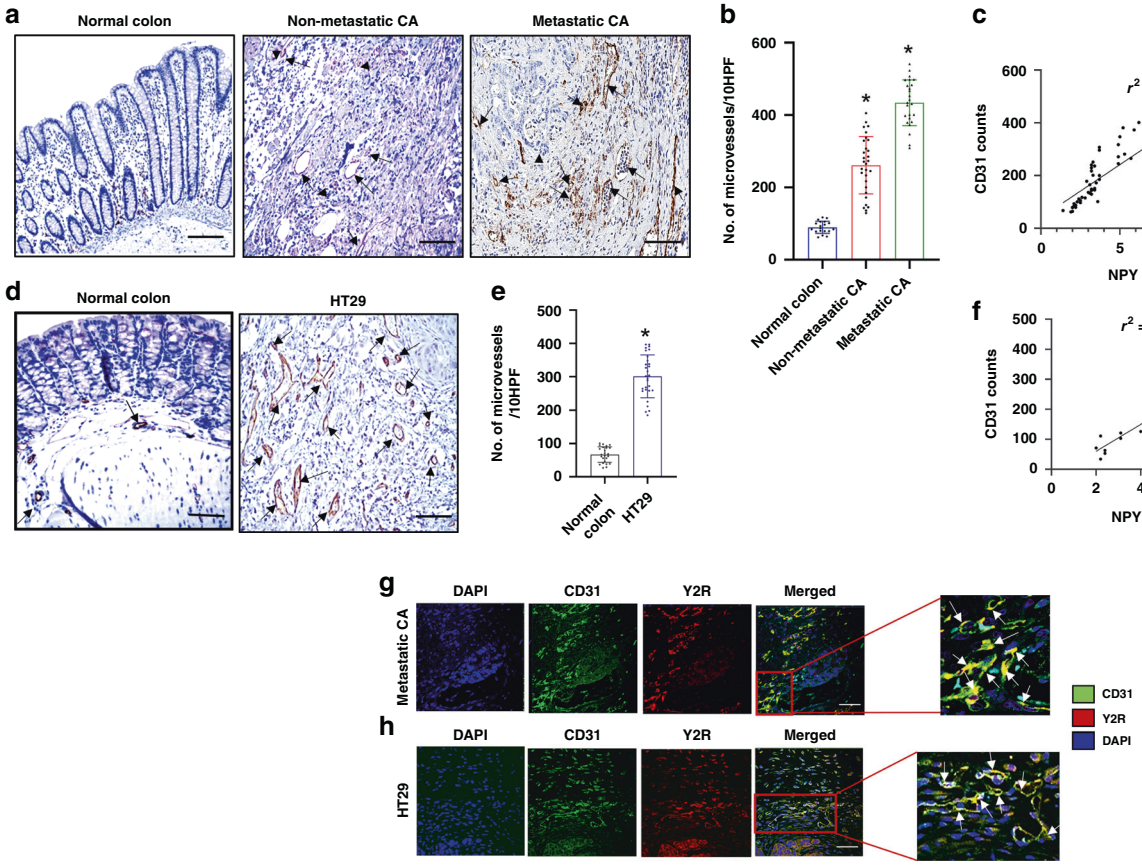

Fig. 3 Significant upregulation of angiogenesis (CD31 + ve vessels) in colon adenocarcinoma shows a strong positive correlation with NPY expression. **a** Representative images of immunohistochemistry showed significantly increased angiogenesis in human colon adenocarcinoma (CA) (non-metastatic and metastatic) compared to the normal colon. $n = 21$ per group. Scale bar, 100 µm. **b** Graphical representation of CD31 + ve microvessels in ten high-power microscopic fields (HPF) of normal human colon, non-metastatic and metastatic CA tissues. **c** Correlation between NPY IHC score and CD31 counts in colon tissues ($r^2 = 0.8397$). **d** Significant upregulation of angiogenesis (CD31 + ve vessels) in orthotopic HT29 tumours. **e** Graphical representation of CD31 + ve microvessels in ten HPF of HT29 tumours and normal colon. Data represent the summary of six or more sections per mouse from each group. **f** Correlation between NPY IHC score and CD31 counts in HT29 tumours ($r^2 = 0.8175$). **g** Representative confocal microscopy images showed high expression of Y2R (red) on CD31 + ve endothelial cells (Green) of blood vessels in human metastatic CA (scale bar, 80 µm; $n = 21$) and **h** orthotopic HT29 colon tumours (scale bar, 80 µm, $n = 11$). Results are expressed as mean ± SEM; $^*P < 0.01$ compared to the normal colon.

CEC, and our in vivo results indicated that treatment with Y2R antagonists inhibited HT29 colon cancer growth by reducing the number of neovessels in the tumours, we therefore next investigated the effect of NPY on angiogenic processes in vitro using CEC. We observed that NPY (100 nM, Tocris) significantly stimulated proliferation (at 24 hrs) (Fig. 5d), mobilization (in vitro transwell cell migration, at 8 hrs) and migration (wound-healing assay, at 20 hrs) of CEC (Fig. 5e, f). However, the effect of NPY on CEC was abrogated when these cells were prior treated with Y2R antagonist BIIE0246 (1 µM, Tocris) or Y2R expression was silenced by siRNA (siY2R) transfection (40 µM) (Fig. 5d–f). Similarly, NPY promoted tubule formation of CEC in vitro as evidenced by increased numbers of tubules per microscopic field (Fig. 5g), increased vessel area coverage and increased tubular branching after 48 hrs of stimulation (Supplementary Fig. S6), which was abolished by either prior treatment of CEC with NPY antagonist or by using siY2R. Western blot analysis confirmed the silencing of Y2R in CEC (Supplementary Fig. S7). However, prior treatment of CEC with the blocker of NPY Y1 receptor (Y1R), BIBO3304 (1 µM, Tocris), failed to stop the proliferation, mobilization and migration or tubule formation of CEC induced by NPY (Fig. 5d–g and Supplementary Fig. S6), thus proving that the stimulatory action of NPY in CEC is mediated specifically through Y2R.

NPY stimulates angiogenesis by activation of the ERK/MAPK pathway

Next, we investigated the molecular mechanism via which NPY-Y2R mediates its action on CEC. Our confocal microscopy results demonstrated that treatment of HT29 colon cancer-bearing mice with Y2R antagonists resulted in decreased angiogenesis in tumour tissues accompanied by reduced expression of both phospho p38 MAPK and phospo p44/42 MAPK in endothelial cells in these tissues (Fig. 6a). To dissect the molecular pathway by which NPY activates angiogenic processes in CEC, we next investigated the status of p38 MAPK and p44/42 MAPK upon NPY stimulation of CEC in vitro. Our western blot results demonstrated that NPY is a potent stimulator of both p38 and p44/42 MAPK in CEC, as, within 5 min of adding NPY to CEC culture, both p38 and p44/42 MAPK were activated. However, this action was inhibited when CEC were pretreated with BIIE0246 (1 µM) (Fig. 6b). To further confirm the role of the ERK/MAPK pathway in the angiogenic processes by NPY, we performed the angiogenic assays (CEC proliferation, migration and tubule formation) with NPY in the presence of two ERK/MAPK inhibitors, SB203580 hydrochloride and FR180204 (1 µM, Tocris). Our results indicated that when CEC were pretreated with either SB203580 hydrochloride or FR180204, NPY failed to promote CEC proliferation, migration and tubule

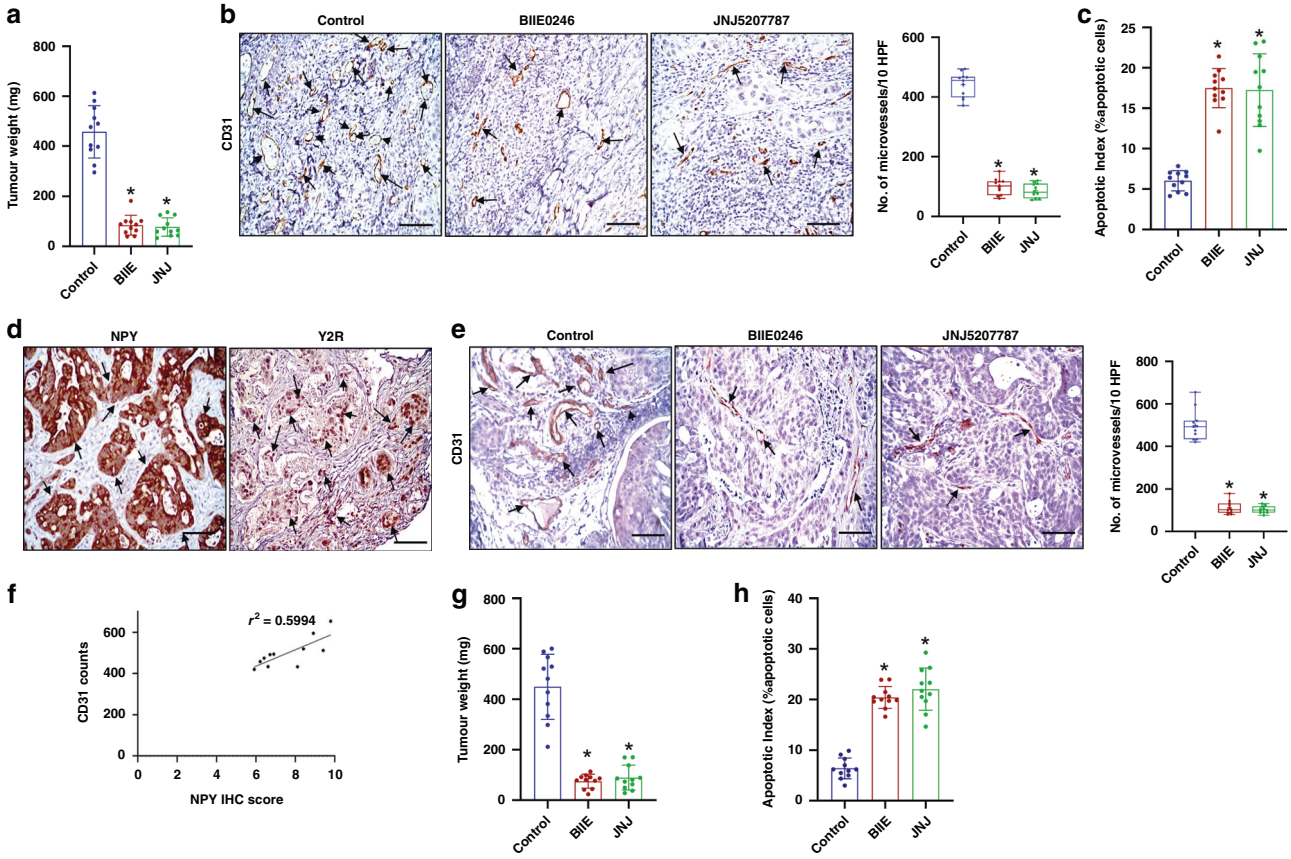

Fig. 4 Significant tumour growth and angiogenesis inhibition upon treatment of orthotopic HT29 and HT29 VEGF-A knockout (VEGF-A KO HT29) tumour-bearing mice with Y2R antagonists, BIIE0246 and JNJ5207787. a HT29 tumour weight was significantly lower in the Y2R antagonists, BIIE0246 and JNJ5207787 treated groups compared to untreated control. $n = 11$ per group. **b** Representative IHC images and graphical representation of the number of CD31 + ve vessels in ten high-power microscopic fields (HPF) showed that angiogenesis was also significantly reduced in HT29 tumours upon treatment with Y2R antagonists. $n = 11$ per group; data represent the summary of six or more sections per mouse from each group. **c** In situ tunnel assay showed a significant increase in tumour cell apoptosis in HT29 tumours upon treatment with Y2R antagonists; data represent the summary of 6 or more sections per mouse from each group. **d** Representative images of IHC showed that both NPY and Y2R are overexpressed in HT29 KO VEGF-A tumours. $n = 11$ per group; data represent the summary of six or more sections per mouse from each group. **e** IHC and graphical representation of the number of CD31 + ve vessels in ten high-power microscopic fields (HPF) indicated that VEGF-A KO HT29 control tumours are highly angiogenic, and angiogenesis is significantly reduced in VEGF-A KO HT29 tumours upon treatment with Y2R antagonists, BIIE0246 and JNJ5207787. **f** Correlation between NPY IHC score and CD31 counts in VEGF-A KO HT29 tumours ($r^2 = 0.5994$). **g** Treatment of orthotopic HT29 KO VEGF-A tumour-bearing mice with Y2R antagonists, BIIE0246 and JNJ5207787, significantly reduced tumour weight. **h** In situ tunnel assay showed a significant increase in tumour cell apoptosis in HT29 KO VEGF-A tumours upon treatment with Y2R antagonists. Results are expressed as mean ± SEM; $^*P < 0.01$ compared to untreated control. Scale bar, 100 μm.

formation (Fig. 5d–g and Supplementary Fig. S6). These results confirmed that NPY promotes angiogenesis in colon cancer via Y2R receptors by activating the ERK/MAPK pathway in CEC.

DISCUSSION

Colorectal cancer is the second leading cause of cancer-related deaths in the United States [41]. Surgery is the conventional first-line treatment for CA, and ~85% of these patients undergo surgery. Patients with unresectable metastatic disease or those at high risk of disease recurrence receive chemotherapy. However, even when the primary tumour is optimally resected, in 50% of these patients, there is tumour recurrence within 5 years of surgery [42, 43]. Furthermore, despite the recent advances in chemotherapy, over 52,000 deaths still occur each year from the disease [42], necessitating the development of newer effective targeted therapies.

Angiogenesis, or the formation of new or neovessels, is a compelling target for therapy because it is an essential process required for the growth and metastasis of many solid tumours, including CA [1, 2, 44]. VEGF-A is the most potent angiogenic factor promoting tumour growth and metastatic dissemination in CA [1, 44, 45]. Anti-VEGF-A agents, combined with chemotherapeutic agents, are used to treat patients with metastatic CA [44, 45]. However, the benefits obtained from the presently used anti-angiogenic agents targeting the actions of VEGF-A are limited, and reports now indicate cases of resistance or non-response to anti-VEGF-A therapy being observed in CA patients. During tumour growth and progression, the formation of blood vessels is a continuous and dynamic process. Inhibiting the VEGF-A pathway stimulates a compensatory biological response by the body, which is manifested by the production of other proangiogenic factors, chemokines and cytokines [8]. Elevations of proangiogenic cytokines, like bFGF, PlGF, and HGF, were observed in some subsets of metastatic CA patients treated with FOLFIRI-bevacizumab in a Phase II study [10]. Other factors providing redundant angiogenic signals pose one of the most critical challenges to the success of anti-VEGF-A therapy by inducing resistance, suggesting that a

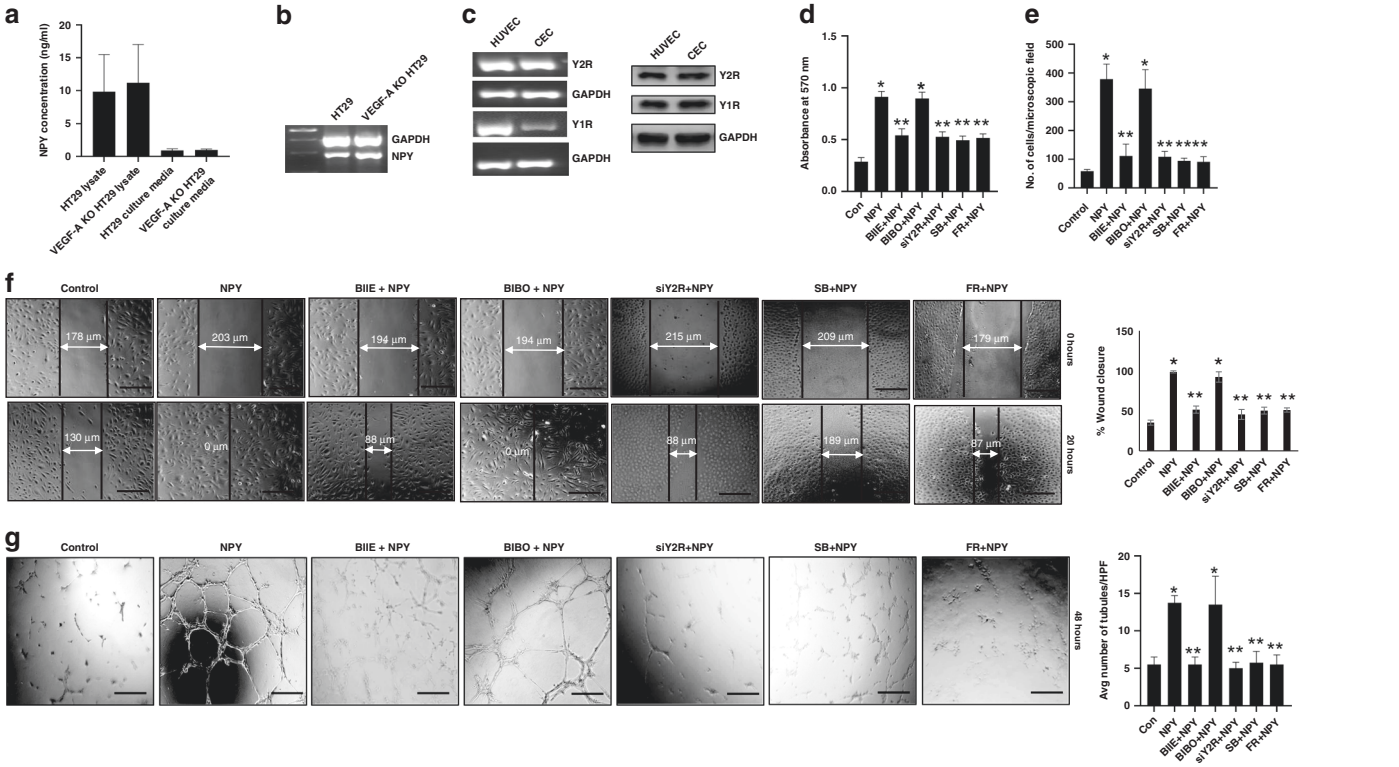

Fig. 5 NPY stimulates the angiogenic potential of colonic endothelial cells via Y2R expressed on these cells. a ELISA assay, and **b** RT-PCR analysis, showed that HT29 and VEGF-A KO HT29 colon cancer cells synthesise and secrete significant amounts of NPY. **c** RT-PCR and western blot analysis indicated the presence of Y2 (Y2R) and Y1 (Y1R) NPY receptors in colonic endothelial cells (CEC) and human umbilical vein endothelial cells (HUVEC). NPY (100 nM) promoted proliferation (**d** MTT assay), mobilization (**e** in vitro transwell migration assay), migration (**f** scratch wound assay) and tubule formation (**g** in vitro tubulogenesis assay) of CEC. Blocking Y2R with BIIE0246 (1 μM) or silencing Y2R (siY2R) in CEC abrogated the effects of NPY. However, the Y1R antagonist, BIBO3304 (1 μM), had no effect on the actions of NPY. Furthermore, pretreatment of CEC with either SB203580 hydrochloride or FR180204 inhibited NPY-induced CEC proliferation, migration and tubule formation. Results are expressed as mean ± SEM; $*P < 0.05$ when compared to control cells and $**P < 0.05$ when compared to NPY-treated cells. Error bars represent SEMs from three independent experiments. Scale bar, 100 μm.

combination of different anti-angiogenic agents could be beneficial in clinical settings.

We have identified and defined NPY as a novel independent regulator of colon cancer angiogenesis using CA samples from patients who presented with metastasis to liver and lymph nodes, adjacent normal/benign tissue, normal colon tissues, orthotopic HT29 xenograft models and a combination of in vivo and in vitro experiments (Figs. 1–5). NPY plays a definitive role in the pathogenesis of IBD. Though IBD increases the risk of developing CA, there is no evidence that NPY plays any role in CA progression. Our findings provide the first evidence that NPY can regulate CA growth by promoting angiogenesis. Most interestingly, our results demonstrate that in VEGF-A-depleted condition simulating VEGF-A non-responsive or resistant CA, NPY was significantly upregulated and promoted angiogenesis and, thereby, tumour growth. Blocking Y2R, therefore, could significantly reduce colon cancer growth (Fig. 4). Although NPY has been previously reported to regulate endothelial cell functions via acting through Y2R and Y5R in human umbilical vein endothelial cells (HUVEC) and dermal endothelial cells [41, 46] but it is now well established that the biological properties of endothelial cells considerably vary in different organs [47, 48]. Our study based on human CEC for the first time to our knowledge indicates that NPY is a potent regulator of CEC functions (Fig. 5) and, by acting through Y2R, promotes angiogenic response in colon cancer. Here, we also provide a mechanistic explanation of how NPY regulates neovessel formation in CA. Our in vivo and in vitro data reveal that the proangiogenic actions of NPY via Y2R are mediated through simultaneous activation of both the p44/42 MAPK and p38 MAPK in CEC. Inhibition of the NPY-Y2R axis results in decreased expression of pERK/pMAPK in CEC as was observed in Y2R antagonist-treated colon cancer compared to untreated tumours (Fig. 6). In addition, our in vitro studies indicate that NPY fails to induce angiogenic events in CEC pretreated with selective ERK/MAPK blockers, thus validating our in vivo results (Fig. 5).

Redundancy in angiogenic signalling due to activation of multiple pathways or alternative growth factor signalling pathways is a major reason for the limited success of currently used anti-VEGF-A therapies. Thus several angiogenic growth factors should be targeted simultaneously or sequentially to overcome this challenge. Identifying new and novel angiogenic endogenous factors that regulate angiogenesis in CA is essential for developing novel and effective anti-angiogenic agents that can be combined with existing therapies for maximum clinical benefits. In recent years, anti-angiogenic agents based on GPCR manipulation have been of interest as many GPCR ligands play active roles in promoting aggressive disease states [49]. In this context, our results, for the first time to our knowledge, indicate that NPY, a GPCR ligand, actively promotes angiogenesis in CA via acting through Y2R. Therefore, using Y2R antagonists alone or adding Y2R antagonists to conventional chemotherapeutic or/and anti-angiogenic treatment regimens in CA that express high levels of NPY can be foreseen as a promising therapeutic strategy in the future.

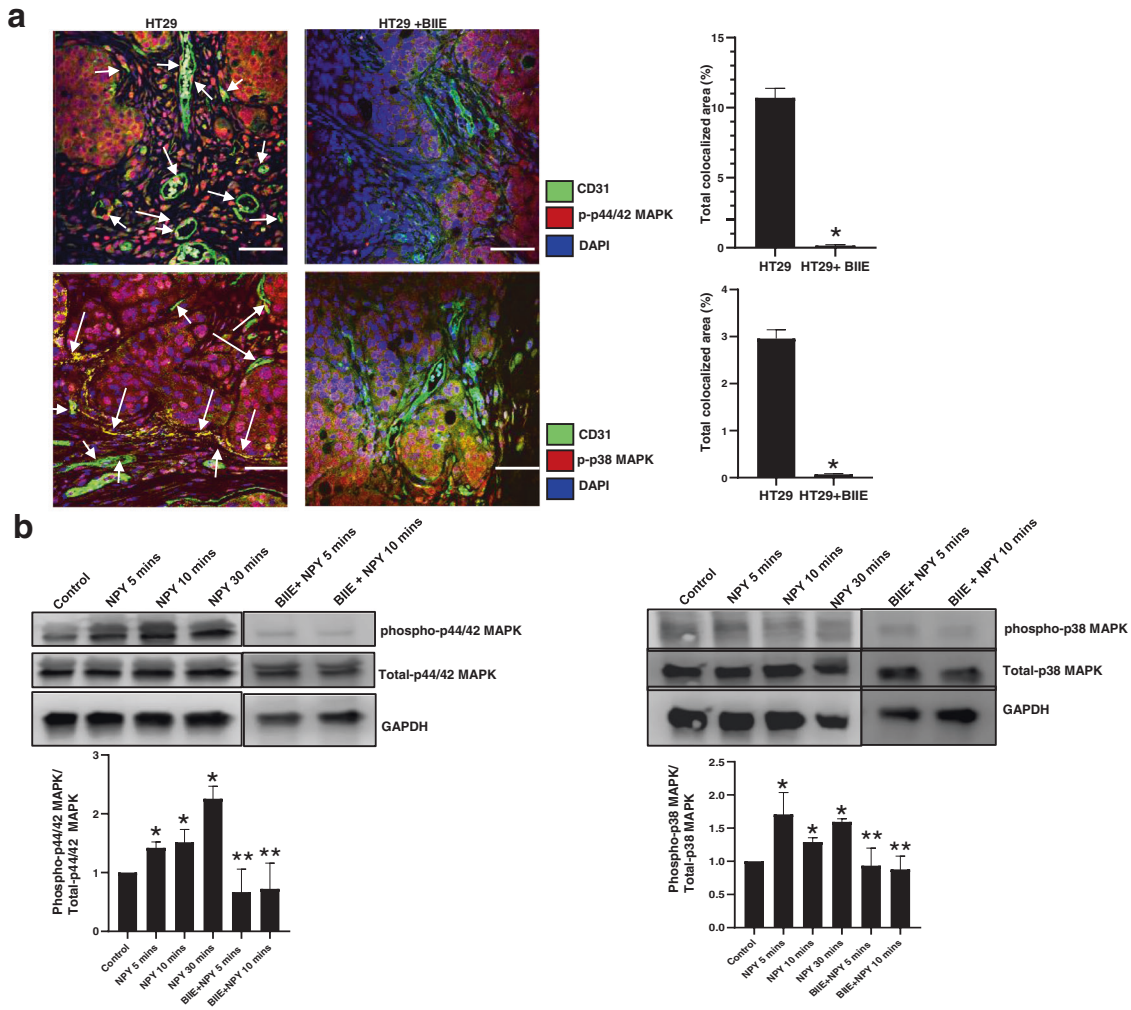

Fig. 6 NPY stimulates angiogenesis in colon cancer by activating the ERK/MAPK pathway. a Representative confocal microscopy images demonstrated that treatment of HT29 colon cancer-bearing mice with Y2R antagonist resulted in decreased expression of phospho p38 MAPK and phospho p44/ 42 MAPK in tumour endothelial cells. $n = 11$; data represent the summary of six or more sections per mouse from each group. **b** Western blot analysis showed that NPY (100 nm) directly and independently activates p38 MAPK as well as p44/42 MAPK in CEC within 5 min upon addition to culture. This activation was abrogated when CEC were pretreated with BIIE0246 (1 μM). Scale bar, 100 μm. Results are expressed as mean ± SEM. $^*P < 0.05$ when compared to control cells and $^{**}P < 0.05$ when compared to NPY-treated cells. Error bars represent SEMs from three independent experiments.

DATA AVAILABILITY

All data relevant to the study are included in the article or uploaded as supplementary information.

REFERENCES

1. Takahashi Y, Kitadai Y, Bucana CD, Cleary KR, Ellis LM. Expression of vascular endothelial growth factor and its receptor, KDR, correlates with vascularity, metastasis, and proliferation of human colon cancer. Cancer Res. 1995;55:3964–8.
2. den Uil SH, van den Broek E, Coupé VMH, Vellinga TT, Delis-van Diemen PM, Bril H, et al. Prognostic value of microvessel density in stage II and III colon cancer patients: a retrospective cohort study. BMC Gastroenterol. 2019;19:146.
3. Ferrara N, Kerbel R. Angiogenesis as a therapeutic target. Nature. 2005;438:967–74.
4. Ferrara N, Adamis A. Ten years of anti-vascular endothelial growth factor therapy. Nat Rev Drug Discov. 2016;15:385–403.
5. Jayson GC, Kerbel R, Ellis LM, Harris AL. Antiangiogenic therapy in oncology: current status and future directions. Lancet. 2016;388:518–29.
6. Itatani Y, Yamamoto T, Zhong C, Molinolo AA, Ruppel J, Hegde P, et al. Suppressing neutrophil-dependent angiogenesis abrogates resistance to anti-VEGF antibody in a genetic model of colorectal cancer. Proc Natl Acad Sci USA. 2020;117:21598–608.
7. Apte RS, Chen DS, Ferrara N. VEGF in signaling and disease: beyond discovery and development. Cell. 2019;176:1248–64.
8. Bergers G, Hanahan D. Modes of resistance to anti-angiogenic therapy. Nat Rev Cancer. 2008;8:592–03.
9. Itatani Y, Kawada K, Yamamoto T, Sakai Y. Resistance to anti-angiogenic therapy in cancer-alterations to anti-VEGF pathway. Int J Mol Sci. 2018;19:1232.
10. Kopetz S, Hoff PM, Morris JS, Wolff RA, Eng C, Glover KY, et al. Phase II trial of infusional fluorouracil, irinotecan, and bevacizumab for metastatic colorectal cancer: efficacy and circulating angiogenic biomarkers associated with therapeutic resistance. J Clin Oncol. 2010;28:453–9.
11. Lakhan SE, Kirchgessner A. Neuroinflammation in inflammatory bowel disease. J Neuroinflammation. 2010;7:37.
12. Duchalais E, Guilluy C, Nedellec S, Touvron M, Bessard A, Touchefeu Y, et al. Colorectal cancer cells adhere to and migrate along the neurons of the enteric nervous system. Cell Mol Gastroenterol Hepatol. 2017;5:31–49.
13. Gamet L, Murat JC, Remaury A, Remesy C, Valet P, Paris H, et al. Vasoactive intestinal peptide and forskolin regulate proliferation of the HT29 human colon adenocarcinoma cell line. J Cell Physiol. 1992;150:501–9.
14. Chandrasekharan B, Bala V, Kolachala VL, Vijay-Kumar M, Jones D, Gewirtz AT, et al. Targeted deletion of neuropeptide Y (NPY) modulates experimental colitis. PLoS ONE. 2008;3:e3304.
15. Dvorak AM, Onderdonk AB, McLeod RS, Monahan-Earley RA, Cullen J, Antonioli DA, et al. Axonal necrosis of enteric autonomic nerves in continent ileal pouches. Possible implications for pathogenesis of Crohn's disease. Ann Surg. 1993;217:260–71.

16. Holzer P, Reichmann F, Farzi A, Neuropeptide Y, peptide YY. and pancreatic polypeptide in the gut-brain axis. Neuropeptides. 2012;46:261–74.
17. Reubi JC, Gugger M, Waser B, Schaer JC. Y(1)-mediated effect of neuropeptide Y in cancer: breast carcinomas as targets. Cancer Res. 2001;61:4636–41.
18. Rasiah KK, Kench JG, Gardiner-Garden M, Biankin AV, Golovsky D, Brenner PC, et al. Aberrant neuropeptide Y and macrophage inhibitory cytokine-1 expression are early events in prostate cancer development and are associated with poor prognosis. Cancer Epidemiol Biomark Prev. 2006;15:711–6.
19. Cox HM. Endogenous PYY and NPY mediate tonic Y1- and Y2-mediated absorption in human and mouse colon. Nutrition. 2008;24:900–6.
20. Hyland NP, Cox HM. The regulation of veratridine-stimulated electrogenic ion transport in mouse colon by neuropeptide Y (NPY), Y1 and Y2 receptors. Br J Pharm. 2005;146:712–22.
21. Rettenbacher M, Reubi JC. Localization and characterization of neuropeptide receptors in human colon. Naunyn Schmiedebergs Arch Pharm. 2001;364: 291–304.
22. Matyal R, Chu L, Mahmood F, Robich MP, Wang A, Hess PE, et al. Neuropeptide Y improves myocardial perfusion and function in a swine model of hypercholesterolemia and chronic myocardial ischemia. J Mol Cell Cardiol. 2012;53:891–8.
23. Novielli NM, Al-Khazraji BK, Medeiros PJ, Goldman D, Jackson DN. Pre-diabetes augments neuropeptide Y1- and α1-receptor control of basal hindlimb vascular tone in young ZDF rats. PLoS ONE. 2012;7:e46659.
24. McDermott BJ, Bell D. NPY and cardiac diseases. Curr Top Med Chem. 2007;7: 1692–703.
25. Velayos F. Colon cancer surveillance in inflammatory bowel disease patients: current and emerging practices. Expert Rev Gastroenterol Hepatol. 2008;2:817–25.
26. Lakatos PL, Lakatos L. Risk for colorectal cancer in ulcerative colitis: changes, causes and management strategies. World J Gastroenterol. 2008;14:3937–47.
27. Feagins LA, Souza RF, Spechler SJ. Carcinogenesis in IBD: potential targets for the prevention of colorectal cancer. Nat Rev Gastroenterol Hepatol. 2009;6:297–305.
28. Sarkar C, Chakroborty D, Goswami S, Fan H, Mo X, Basu S. VEGF-A controls the expression of its regulator of angiogenic functions, dopamine D2 receptors on endothelial cells. J Cell Sci. 2022; https://doi.org/10.1242/jcs.259617.
29. Chakroborty D, Sarkar C, Yu H, Wang J, Liu Z, Dasgupta PS, et al. Dopamine stabilizes tumor blood vessels by upregulating angiopoietin 1 expression in pericytes and Kruppel-like factor-2 expression in tumor endothelial cells. Proc Natl Acad Sci USA. 2011;108:20730–5.
30. Sarkar C, Chakroborty D, Chowdhury UR, Dasgupta PS, Basu S. Dopamine increases the efficacy of anticancer drugs in breast and colon cancer preclinical models. Clin Cancer Res. 2008;14:2502–10.
31. Janssen P, Verschueren S, Rotondo A, Tack J. Role of Y(2) receptors in the regulation of gastric tone in rats. Am J Physiol Gastrointest Liver Physiol. 2012;302:G732–9.
32. Mittapalli GK, Roberts E. Ligands of the neuropeptide Y Y2 receptor. Bioorg Med Chem Lett. 2014;24:430–41.
33. Fedchenko N, Reifenrath J. Different approaches for interpretation and reporting of immunohistochemistry analysis results in the bone tissue—a review. Diagn Pathol. 2014;9:221.
34. Chakroborty D, Sarkar C, Mitra RB, Banerjee S, Dasgupta PS, Basu S. Depleted dopamine in gastric cancer tissues: dopamine treatment retards growth of gastric cancer by inhibiting angiogenesis. Clin Cancer Res. 2004;10:4349–56.
35. Chakroborty D, Chowdhury UR, Sarkar C, Baral R, Dasgupta PS, Basu S. Dopamine regulates endothelial progenitor cell mobilization from mouse bone marrow in tumor vascularization. J Clin Investig. 2008;118:1380–9.
36. Sarkar C, Ganju RK, Pompili VJ, Chakroborty D. Enhanced peripheral dopamine impairs post-ischemic healing by suppressing angiotensin receptor type 1 expression in endothelial cells and inhibiting angiogenesis. Angiogenesis. 2017;20:97–107.
37. Lu K, Chakroborty D, Sarkar C, Lu T, Xie Z, Liu Z, et al. Triphala and its active constituent chebulinic acid are natural inhibitors of vascular endothelial growth factor-a mediated angiogenesis. PLoS ONE. 2012;7:e43934.
38. Basu S, Sarkar C, Chakroborty D, Nagy J, Mitra RB, Dasgupta PS, et al. Ablation of peripheral dopaminergic nerves stimulates malignant tumor growth by inducing vascular permeability factor/vascular endothelial growth factor-mediated angiogenesis. Cancer Res. 2004;64:5551–5.
39. Sarkar C, Das S, Chakroborty D, Chowdhury UR, Basu B, Dasgupta PS, et al. Cutting edge: stimulation of dopamine D4 receptors induce T cell quiescence by upregulating Kruppel-like factor-2 expression through inhibition of ERK1/ERK2 phosphorylation. J Immunol. 2006;177:7525–9.
40. Aerts E, Geets E, Sorber L, Beckers S, Verrijken A, Massa G, et al. Evaluation of a role for NPY and NPY2R in the pathogenesis of obesity by mutation and copy number variation analysis in obese children and adolescents. Ann Hum Genet. 2018;82:1–10.
41. Movafagh S, Hobson JP, Spiegel S, Kleinman HK, Zukowska Z. Neuropeptide Y induces migration, proliferation, and tube formation of endothelial cells bimodally via Y1, Y2, and Y5 receptors. FASEB J. 2006;20:1924–6.
42. Siegel RL, Miller KD, Fuchs HE, Jemal A. Cancer statistics, 2021. CA Cancer J Clin. 2021;71:7–33.
43. Chibaudel B, Tournigand C, André T, de Gramont A. Therapeutic strategy in unresectable metastatic colorectal cancer. Ther Adv Med Oncol. 2012;4:75–89.
44. Sun W. Angiogenesis in metastatic colorectal cancer and the benefits of targeted therapy. J Hematol Oncol. 2012;5:63.
45. Lopez A, Harada K, Vasilakopoulou M, Shanbhag N, Ajani JA. Targeting angiogenesis in colorectal carcinoma. Drugs. 2019;79:63–74.
46. Silva AP, Kaufmann JE, Vivancos C, Fakan S, Cavadas C, Shaw P, et al. Neuropeptide Y expression, localization and cellular transducing effects in HUVEC. Biol Cell. 2005;97:457–67.
47. Lacorre DA, Baekkevold ES, Garrido I, Brandtzaeg P, Haraldsen G, Amalric F, et al. Plasticity of endothelial cells: rapid dedifferentiation of freshly isolated high endothelial venule endothelial cells outside the lymphoid tissue microenvironment. Blood. 2004;103:4164–72.
48. Aird WC. Phenotypic heterogeneity of the endothelium: I. Structure, function, and mechanisms. Circ Res. 2007;100:158–73.
49. De Francesco EM, Sotgia F, Clarke RB, Lisanti MP, Maggiolini M. G protein-coupled receptors at the crossroad between physiologic and pathologic angiogenesis: old paradigms and emerging concepts. Int J Mol Sci. 2017;18:2713.

ACKNOWLEDGEMENTS

We acknowledge the support of the veterinarian and vivarium staff of OSU ULAR for our animal studies and OSU Pathology Core facilities for confocal microscopy studies.

AUTHOR CONTRIBUTIONS

Conception: CS; design: CS, DC and SG; development of methodology: DC, SG and CS; experiment and data generation: DC, SG and HF; analysis and interpretation of data: CS, DC, SG, HF, WF and SB; writing original draft: DC, SG and CS; writing/reviewing and editing: DC, SG, HF, WF, SB and CS; administrative and study supervision: DC and CS. All authors read and approved the final manuscript.

FUNDING

This study was supported by funding from NIH/NCI [R21 CA216763 to CS]. CS and DC would like to acknowledge the funding received from Mitchell Cancer Institute, University of South Alabama. DC was also supported by DOD, USA [W81XWH-20-1-0618], and SB was supported by DOD, USA [W81XWH-19-1-0233 and W81XWH2110874].

COMPETING INTERESTS

The authors declare no competing interests.

ETHICS APPROVAL AND CONSENT TO PARTICIPATE

Only de-identified and archived human colon cancer tissues were used under an exempt (category 4) protocol as determined by The Ohio State University Institutional Review Board. The study was performed in accordance with the Declaration of Helsinki.

CONSENT TO PUBLISH

Not applicable.

ADDITIONAL INFORMATION

Supplementary information The online version contains supplementary material available at https://doi.org/10.1038/s41416-022-01916-1.

Correspondence and requests for materials should be addressed to Chandrani Sarkar.

Reprints and permission information is available at http://www.nature.com/reprints

Publisher's note Springer Nature remains neutral with regard to jurisdictional claims in published maps and institutional affiliations.